Christian Constanda
Bardo E. J. Bodmann
Paul J. Harris
Editors

Integral Methods in Science and Engineering

Applications in Theoretical and Practical Research

Birkhäuser

Birkhäuser

Christian Constanda • Bardo E. J. Bodmann •
Paul J. Harris
Editors

Integral Methods in Science and Engineering

Applications in Theoretical and Practical Research

Birkhäuser

Editors
Christian Constanda
Department of Mathematics
The University of Tulsa
Tulsa, OK, USA

Bardo E. J. Bodmann
Engineering School
Federal University of Rio Grande do Sul
Porto Alegre, Rio Grande do Sul, Brazil

Paul J. Harris
Department of Mathematics
University of Brighton
Brighton, UK

ISBN 978-3-031-07170-6 ISBN 978-3-031-07171-3 (eBook)
https://doi.org/10.1007/978-3-031-07171-3

Mathematics Subject Classification: 45Exx, 45E10, 65R20, 45D05

This book is published under the imprint Birkhäuser, www.birkhauser-science.com by the registered company Springer Nature Switzerland AG
The registered company address is: Gewerbestrasse 11, 6330 Cham, Switzerland

Preface

The international conferences on Integral Methods in Science and Engineering (IMSE) started in 1985 at the University of Texas–Arlington, and continued biennially in a variety of venues around the world, bringing together specialists who employ integration techniques as essential tools in their research. These procedures exhibit generality, elegance, and efficiency, all of which are essential ingredients in the work of a wide category of practitioners.

The dates and venues of the first 15 IMSE conferences are listed below.

1985, 1990: University of Texas–Arlington, TX, USA
1993: Tohoku University, Sendai, Japan
1996: University of Oulu, Finland
1998: Michigan Technological University, Houghton, MI, USA
2000: Banff, AB, Canada (organized by the University of Alberta, Edmonton)
2002: University of Saint-Étienne, France
2004: University of Central Florida, Orlando, FL, USA
2006: Niagara Falls, ON, Canada (organized by the University of Waterloo)
2008: University of Cantabria, Santander, Spain
2010: University of Brighton, UK
2012: Bento Gonçalves, Brazil (organized by the Federal University of Rio Grande do Sul)
2014: Karlsruhe Institute of Technology, Germany
2016: University of Padova, Italy
2018: University of Brighton, UK

Due to the unfavorable world health conditions, the 2020 conference, scheduled to be held at the Steklov Mathematical Institute in St. Petersburg, Russia, had to be postponed. However, as an intermediate solution, a Symposium on the Theory and Applications of Integral Methods in Scientific Research was held online in July 2021. By making public their latest results, the participants in this event, all with long-standing IMSE credentials, have kept the flames of our common research interests burning bright, in anticipation of the more inclusive in-person meeting expected to take place, as planned, in St. Petersburg in the summer of 2022.

The peer-reviewed chapters of this volume, arranged alphabetically by first author's name, consist of 22 of the papers presented at the 2021 symposium. The editors would like to thank the reviewers for their help, Christopher Tominich at Birkhäuser–New York for his support of this project, and Saveetha Balasundaram and her production team for their courteous and professional handling of the publication process.

Tulsa, OK, USA — Christian Constanda
Porto Alegre, Brazil — Bardo E. J. Bodmann
Brighton, UK — Paul J. Harris
January 2022

The International Steering Committee of IMSE

Contents

Contributors

Luiz Felipe Fracasso Chaves Barcellos Nuclear Studies Group, School of Engineering, Federal University of Rio Grande do Sul, Porto Alegre, RS, Brazil

Ricardo Carvalho de Barros University of the State of Rio de Janeiro, Polytechnic Institute, Nova Friburgo, RJ, Brazil

Wagner Queiroz Barros Laboratory of Petroleum Engineering and Exploration, State University of Northern Rio de Janeiro, Macaé, RJ, Brazil

Daniel Gustavo Benvenutti Nuclear Studies Group, School of Engineering, Federal University of Rio Grande do Sul, Porto Alegre, RS, Brazil

Luiz Fernando Bez Institute of Computing, Federal Fluminense University, Noterói, RJ, Brazil

Bardo Ernst Josef Bodmann Postgraduate Program in Mechanical Engineering, School of Engineering, Federal University of Rio Grande do Sul, Porto Alegre, RS, Brazil

Daniela Buske Department of Mathematics and Statistics, Institute of Physics and Mathematics, Federal University of Pelotas, Capão do Leão, RS, Brazil

David Chappell Department of Physics and Mathematics, Nottingham Trent University, Nottingham, UK

Christian Constanda Department of Mathematics, The University of Tulsa, Tulsa, OK, USA

Leonardo Rodrigues da Costa Moraes University of the State of Rio de Janeiro, Polytechnic Institute, Nova Friburgo, RJ, Brazil

Mulugeta Alemayehu Dagnaw Department of Mathematics, Debre Tabor University, Debre Tabor, Ethiopia

Dale R. Doty Department of Mathematics, The University of Tulsa, Tulsa, OK, USA

Camila Fávero Department of Mathematics and Statistics, Institute of Physics and Mathematics, Federal University of Pelotas, Capão do Leão, RS, Brazil

Júlio César Lombaldo Fernandes Institute of Mathematics and Statistics, Federal University of Rio Grande do Sul, Porto Alegre, RS, Brazil

Débora Lídia Gisch Institute of Mathematics and Statistics, Federal University of Rio Grande do Sul, Porto Alegre, RS, Brazil

Delfina Gómez Departamento Matemáticas, Estadística y Computación, Facultad de Ciencias, Universidad de Cantabria, Santander, Spain

Glénio Aguiar Gonçalves Department of Mathematics and Statistics, Institute of Physics and Mathematics, Federal University of Pelotas, Capão do Leão, RS, Brazil

Evgeny A. Gorodnitskiy St. Petersburg State University, St. Petersburg, Russia

Igor A. Guz School of Engineering, University of Aberdeen, Aberdeen, UK

Paul J. Harris University of Brighton, School of Architecture, Technology and Engineering, Brighton, UK

Andreas Kleefeld Jülich Supercomputing Centre, Forschungszentrum Jülich GmbH, Jülich, Germany

Renato Aloisio dos Santos Klein Institute of Mathematics and Statistics, Federal University of Rio Grande do Sul, Porto Alegre, RS, Brazil

Cibele Aparecida Ladeia Institute of Mathematics and Statistics, Federal University of Rio Grande do Sul, Porto Alegre, RS, Brazil

Rogério José Marczak Mechanical Engineering Department, School of Engineering, Federal University of Rio Grande do Sul, Porto Alegre, RS, Brazil

André Meneghetti Institute of Mathematics, Statistics and Physics, Federal University of Rio Grande, Rio Grandev, RS, Brazil

Oleksandr Menshykov School of Engineering, University of Aberdeen, Aberdeen, UK

Marina Menshykova School of Engineering, University of Aberdeen, Aberdeen, UK

Sergey E. Mikhailov Brunel University London, Department of Mathematics, Uxbridge, UK

Dorina Mitrea Department of Mathematics, Baylor University, Waco, TX, USA

Irina Mitrea Department of Mathematics, Temple University, Philadelphia, PA, USA

Marius Mitrea Department of Mathematics, Baylor University, Waco, TX, USA

Ram S. Mohan Department of Mechanical Engineering, The University of Tulsa, Tulsa, OK, USA

Sergey A. Nazarov Faculty of Mathematics and Mechanics, St. Petersburg State University, St. Petersburg, Russia
Institute of Problems of Mechanical Engineering RAS, St. Petersburg, Russia

Rafael Orive-Illera Departamento de Matemáticas, Facultad de Ciencias, Universidad Autónoma de Madrid, Madrid, Spain
Instituto de Ciencias Matemáticas, CSIC-UAM-UC3M-UCM, Madrid, Spain

Aline R. Parigi Federal Institute of Education, Science and Technology Farroupilha, São Vicente do Sul, RS, Brazil

Maria V. Perel St. Petersburg State University, St. Petersburg, Russia

Álvaro Marcello Marco Peres Laboratory of Petroleum Engineering and Exploration, State University of Northern Rio de Janeiro, Macaé, RJ, Brazil

Maria-Eugenia Pérez-Martínez Departamento Matemática Aplicada y Ciencias de la Computación, ETSI Caminos, Universidad de Cantabria, Santander, Spain

Adolfo Puime Pires Laboratory of Petroleum Engineering and Exploration, State University of Northern Rio de Janeiro, Macaé, RJ, Brazil

Carlos Fresneda-Portillo Department of Quantitative Methods, Universidad Loyola Andalucía, Dos Hermanas, Sevilla, Spain

Régis Sperotto de Quadros Department of Mathematics and Statistics, Institute of Physics and Mathematics, Federal University of Pelotas, Capão do Leão, RS, Brazil

Jacob Rowbottom Department of Physics and Mathematics, Nottingham Trent University, Nottingham, UK

Jean Schmith Polytechnic School, University of Vale do Rio dos Sinos, São Leopoldo, RS, Brazil

Marcelo Schramm Center of Engineering, Federal University of Pelotas, Pelotas, RS, Brazil

Adalberto Schuck Jr. Department of Electrical Engineering, School of Engineering, Federal University of Rio Grande do Sul, Porto Alegre, RS, Brazil

Cynthia Feijó Segatto Institute of Mathematics and Statistics, Federal University of Rio Grande do Sul, Porto Alegre, RS, Brazil

Malay Jignesh Shah Department of Mechanical Engineering, The University of Tulsa, Tulsa, OK, USA

Ovadia Shoham Department of Petroleum Engineering, The University of Tulsa, Tulsa, OK, USA

Fernando Carvalho da Silva Department of Nuclear Engineering, Federal University of Rio de Janeiro, Centro de Tecnologia, Rio de Janeiro, RJ, Brazil

Fernanda Tumelero Graduate Program in Mechanical Engineering, School of Engineering, Federal University of Rio Grande do Sul, Porto Alegre, RS, Brazil

Marco Tullio Menna Barreto de Vilhena Graduate Program in Mechanical Engineering, School of Engineering, Federal University of Rio Grande do Sul, Porto Alegre, RS, Brazil

Heloisa Robattini Zanetti Institute of Mathematics and Statistics, Federal University of Rio Grande do Sul, Porto Alegre, RS, Brazil

Haoqing Zhao Department of Petroleum Engineering, The University of Tulsa, Tulsa, OK, USA

Maria Zimmermann Medical Engineering and Technomathematics, FH Aachen Campus Jülich, Jülich, Germany

Chapter 1
Approximate Solution for One-Dimensional Compressible Two-Phase Immiscible Flow in Porous Media for Variable Boundary Conditions

W. Q. Barros, A. P. Pires, and Á. M. M. Peres

1.1 Introduction

In most petroleum reservoirs, there are at least two phases: oil and connate water. Usually, water is also injected to increase oil production and keep the reservoir pressure at some desired level. Oil displacement by injected water can be modeled by a system of two partial differential equations representing the mass conservation of each component and Darcy's law replacing momentum balance. For one-dimensional incompressible systems without mass transfer, the problem can be solved by the method of characteristics [BL42]. If the relative permeability curves are convex, the solution is given by a continuous two-phase saturation zone (rarefaction wave) followed by a discontinuity (shock). This solution was further expanded to include gravitational and capillary effects [SC59, FS59], to evaluate the pressure drop along porous medium [W52, JBN59], and for three-phase flow [IMPT92, GF97, AS09, CAFM16]. Analytical solutions for compressible two-phase problems are more difficult to develop because both pressure and saturation fields must be solved simultaneously. Approximate solutions were obtained for a two-zone system with constant saturation in each zone [HRM58, KMJ72]. Splitting the two-phase region in more segments improves the accuracy of the solution. The water saturation in each zone of this multi-region system is constant, and thus the velocity of water saturation front in the pressure solution can be neglected and a quasi-static approach can be used [AK89]. The authors of [BH90] proposed a different approximate solution superposing pressure transient effects on a previous saturation profile obtained by Buckley–Leverett solution. The authors of [TR97] generalized the theory for multiphase flow in a heterogeneous reservoir. In this approach, the

W. Q. Barros · A. P. Pires (✉) · Á. M. M. Peres
Universidade Estadual do Norte Fluminense, Macaé, RJ, Brazil
e-mail: adolfo.puime@gmail.com; alvaroperes@lenep.uenf.br

C. Constanda et al. (eds.), *Integral Methods in Science and Engineering*,
https://doi.org/10.1007/978-3-031-07171-3_1

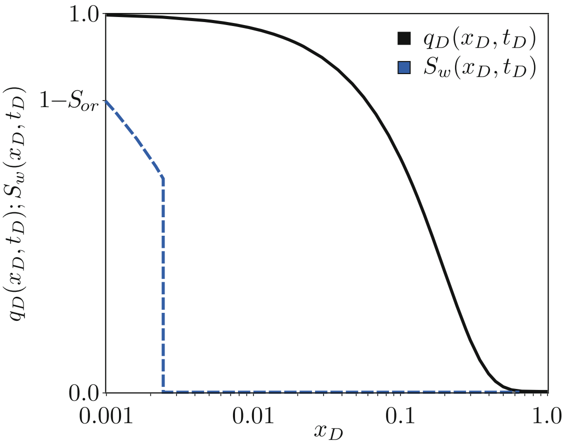

Fig. 1.1 Typical water saturation and dimensionless flow rate profiles for constant injection rate for a fixed time

pressure and saturation zones move with different velocities, in which the saturation front is always within a steady-state flow-rate zone (Fig. 1.1). It is a simplified method to calculate the pressure profile for the problem of constant fluid injection, in which the saturation is obtained by the immiscible Buckley–Leverett problem and the flow rate by the single-phase compressible solution. The pressure solution is calculated integrating Darcy's equation [BTR98, PR03, PBR04, PBR06].

For constant boundary conditions, the Thompson–Reynolds conjecture provides good results when compared to numerical experiments. However, for non-constant boundary conditions, a new pressure perturbation along the reservoir appears and the conjecture cannot be applied. In this work, we present a new procedure to generalize the solution for non-constant boundary conditions. In Sect. 1.2, we derive the mathematical formulation and present an approximate solution. Next, we compare the solution with numerical results under different injection schedules and system compressibility (1.3). Finally, some conclusions are addressed (1.4).

1.2 Mathematical Model

In this work, it is considered a one-dimensional oil displacement by water in a homogeneous porous medium (Fig. 1.2). Additional hypothesis are:

- Immiscible and isothermal linear flow
- Constant cross-sectional area
- Negligible dispersion, gravitational and capillary effects
- Constant viscosity phases
- Constant phases and rock compressibility
- Darcy's law is valid

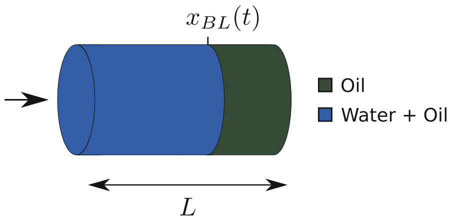

Fig. 1.2 Representation of 1D water flooding

The velocity of each phase can be calculated using Darcy's law,

$$v_\pi = -\frac{Kk_{r\pi}}{\mu_\pi}\frac{\partial P}{\partial x} \ , \tag{1.1}$$

where K and $k_{r\pi}$ are the absolute and phase relative permeabilities, μ_π the phase viscosity, and $\frac{\partial P}{\partial x}$ the linear pressure gradient; the subscript π denotes water w or oil o phase. Summing up the velocity for all phases and neglecting capillary effects, one gets

$$q_T(x,t) = -AK\lambda_T(x,t)\frac{\partial P(x,t)}{\partial x} \ , \tag{1.2}$$

where A is the cross-sectional area, q_T represents the total volumetric flow rate, and λ_T is the total mobility of the phases ($\lambda_T = \frac{k_{rw}}{\mu_w} + \frac{k_{ro}}{\mu_o}$).

To determine the pressure profile along the porous medium length, we integrate Eq. 1.2 using a constant pressure external boundary condition

$$P(x = L, t) = P_i \ ,$$

in which P_i denotes the initial pressure and L is the core length, resulting in

$$P(x,t) - P_i = \frac{1}{AK}\int_x^L \frac{q_T(x',t)}{\lambda_T(x',t)}dx'.$$

Now, we introduce dimensionless time and space coordinates,

$$x_D = \frac{x}{L} \ , \tag{1.3}$$

$$t_D = \frac{q_{ref}\ t}{(1 - S_{wi} - S_{or})\,AL\phi} \ , \tag{1.4}$$

where q_{ref} is a reference flow rate, adopted as the first injection value, and ϕ is the rock porosity. The irreducible water saturation and residual oil saturation are denoted by S_{wi} and S_{or}, respectively. Thus, the pressure drop can be written in dimensionless variables as

$$P_D\left(x_D, t_D\right) = \int_{x_D}^{1} \frac{q_D\left(x'_D, t_D\right)}{\lambda_{TD}\left(x'_D, t_D\right)} dx'_D \,, \tag{1.5}$$

where

$$P_D\left(x_D, t_D\right) = \frac{KA\hat{\lambda}_o}{q_{ref}L}\left(P\left(x, t\right) - P_i\right) \,, \tag{1.6}$$

$$\lambda_{TD}\left(x_D, t_D\right) = \frac{\lambda_T\left(x, t\right)}{\hat{\lambda}_o} \,, \tag{1.7}$$

$$q_D\left(x_D, t_D\right) = \frac{q_T\left(x, t\right)}{q_{ref}} \,, \tag{1.8}$$

in which $\hat{\lambda}_o$ is oil mobility at water irreducible saturation. Equation 1.5 relates the flow rate and mobility profiles to the pressure drop change at a given position x_D. In this work, we solve this problem for the case of step-change internal boundary condition. Thus, an approximation can be obtained based on two key hypotheses:

1. The mobility profile can be obtained by the incompressible problem solution.
2. The total flow rate can be calculated considering two regions with fixed interface position for compressible flow.

The total flow rate is obtained from a linear partial differential equation. Thus, Eq. 1.5 applied for the internal boundary condition $P_D\left(x_D = 0, t_D\right) = P_{wD}\left(t_D\right)$ is written as

$$P_{wD}\left(t_D\right) = \int_{0}^{1} \frac{q_D\left(x'_D, t_D\right)}{\lambda_{TD}\left(x'_D, t_D\right)} dx'_D \,, \tag{1.9}$$

where

$$q_D\left(x_D, t_D\right) = \sum_{j=1}^{Nsteps} \left[q_{D_j}^{Inj} - q_{D_{j-1}}^{Inj}\right] q_{DC}\left(x_D, t_D - t_{D_{j-1}}\right) \,.$$

The last equation is the flow-rate superposition, in which $Nsteps$ is the number of flow-rate steps until t_D, $q_{D_j}^{Inj}$ is the injection flow rate in step j, and t_{D_j} is the time when $q_{D_j}^{Inj}$ started. The terms inside parenthesis are the (x_D, t_D) coordinates where q_{DC} and λ_{TD} are evaluated. The function q_{DC} is the mathematical solution for the two-region problem under constant injection rate.

1.2.1 Approximation for $\lambda_{TD}(x_D, t_D)$

The mass conservation for simultaneous flow of oil and water in a linear porous media is modeled by the equations

$$\frac{\partial\left(\phi S_\pi \rho_\pi\right)}{\partial t} + \frac{\partial\left(\rho_\pi v_\pi\right)}{\partial x} = 0,\ \pi = w, o\ , \tag{1.10}$$

where ρ_π is the phase density. Considering an incompressible system, we find

$$\frac{\partial S_\pi}{\partial t} + \frac{1}{\phi}\frac{\partial v_\pi}{\partial x} = 0,\ \pi = w, o\ .$$

Defining the normalized water saturation as

$$S_{nw} = \frac{S_w - S_{wi}}{1 - S_{wi} - S_{or}},\ S_w \in \left[S_{wi}, 1 - S_{or}\right]$$

and applying the definitions of dimensionless variables (Eqs. 1.3, 1.4, and 1.8) together with Darcy's law (Eq. 1.1), we find [BL42]

$$\frac{\partial S_{nw}}{\partial t_D} + q_D\left(x_D = 0, t_D\right)\frac{\partial f_w}{\partial x_D} = 0\ ,$$

in which f_w defines the water fractional flow

$$f_w = \frac{\frac{k_{rw}}{\mu_w}}{\frac{k_{rw}}{\mu_w} + \frac{k_{ro}}{\mu_o}}\ .$$

For convex relative permeability curves, the derivative $\frac{df_w}{dS_{nw}}$ is not monotonic and the solution is not unique. To determine the most admissible solution, we apply the Lax [L57] and Oleinik [O57] stability criteria, and the solution is composed of a rarefaction wave followed by a shock. The shock must be a zero-diffusion limit of the solution given by traveling waves [L07]. The solution is given by

$$S_{nw} = \begin{cases} \frac{df_w}{dS_{nw}}^{-1}\left(\frac{1}{q_D(x_D=0,t_D)}\frac{x_D}{t_D}\right), & x_D \in \left(0, x_D^{BL}\right)\ , \\ 0, & x_D \in \left(x_D^{BL}, 1\right)\ , \end{cases} \tag{1.11}$$

where $\left(\frac{1}{q_D(x_D=0,t_D)}\frac{x_D}{t_D}\right)$ is the self-similar variable where the inverse of $\frac{df_w}{dS_{nw}}$ is evaluated. The shock position is denoted by x_D^{BL} (Fig. 1.2) and is calculated solving the Rankine–Hugoniot ODE condition.

$$\frac{dx_D^{BL}}{dt_D} = q_D\left(x_D = 0, t_D\right)\frac{f_w^{BL}}{S_{nw}^{BL}}.$$

1.2.2 Approximation for $q_{DC}(x_D, t_D)$

Applying Darcy's law (Eq. 1.1) in the mass conservation (Eq. 1.10), we find

$$S_\pi \left(\phi \frac{\partial \rho_\pi}{\partial P} + \rho_\pi \frac{\partial \phi}{\partial P} \right) \frac{\partial P}{\partial t} + (\phi \rho_\pi) \frac{\partial S_\pi}{\partial t} - \left(\rho_\pi \frac{\partial \left(\frac{K k_{r\pi}}{\mu_\pi} \frac{\partial P}{\partial x} \right)}{\partial x} + \frac{K k_{r\pi}}{\mu_\pi} \frac{\partial \rho_\pi}{\partial P} \left(\frac{\partial P}{\partial x} \right)^2 \right) = 0, \;\; \pi = w, o \tag{1.12}$$

Using the rock and fluid compressibility definitions ($c_\phi = \frac{1}{\phi}\frac{\partial \phi}{\partial P}$ and $c_\pi = \frac{1}{\rho_\pi}\frac{\partial \rho_\pi}{\partial P}$) and summing for both phases, it is possible to derive

$$\frac{\partial \left(\lambda_T \frac{\partial P}{\partial x} \right)}{\partial x} + (c_w \lambda_w + c_o \lambda_o) \left(\frac{\partial P}{\partial x} \right)^2 = \frac{\phi c_t}{K} \frac{\partial P}{\partial t} \; ,$$

where c_t is the total compressibility, given by

$$c_t(x, t) = c_\phi + c_o (1 - S_w(x, t)) + c_w S_w(x, t) \, .$$

For small pressure gradients and slightly compressible fluids, the quadratic term can be neglected. Thus, applying the dimensionless definitions (Eqs. 1.3, 1.4, and 1.5), we find the dimensionless PDE for the pressure in a compressible two-phase system,

$$\frac{1}{\lambda_{TD}} \frac{\partial \left(\lambda_{TD} \left(\frac{\partial P_D}{\partial x_D} \right) \right)}{\partial x_D} = \gamma_L \frac{\partial P_D}{\partial t_D} \; ,$$

where the term γ_L is given by

$$\gamma_L(x_D, t_D) = \frac{q_{ref} L}{(1 - S_{wi} - S_{or}) K A} \frac{c_t}{\lambda_T} \, .$$

The terms γ_L and λ_{TD} depend on the saturation profile. To solve this equation, the domain is divided into two regions based on the shock position, and the saturation profile is considered constant in both zones

$$\begin{cases} \frac{\partial^2 P'_D}{\partial x_D^2} = \gamma_L^{IN} \frac{\partial P'_D}{\partial t_D}, & x_D \in \left(0, x_D^{BL}\right) \; , \\ \frac{\partial^2 P'_D}{\partial x_D^2} = \hat{\gamma}_L \frac{\partial P'_D}{\partial t_D}, & x_D \in \left(x_D^{BL}, 1\right) \; , \end{cases}$$

where γ_L^{IN} is the average gamma in the region behind the shock, and $\hat{\gamma}_L$ is the gamma in the original oil condition. Note that P' indicates the pressure for the two-zone problem. The internal boundary condition (I.B.C.) in dimensionless variables is given by

$$\lim_{x_D \to 0}\left(\frac{\partial P'_D}{\partial x_D}\right) = -\frac{1}{\lambda_{TD}^{IN}} \text{ (I.B.C.)} .$$

The initial condition (I.C.) and external boundary condition (E.B.C.) are

$$P'_D\left(x_D = 1, t_D\right) = 0 \text{ (E.B.C.)} ,$$

$$P'_D\left(x_D, t_D = 0\right) = 0 \text{ (I.C)} .$$

Thus, the equations that model the pressure in the inner zone are given by

$$\begin{cases} \frac{\partial^2 P'_D}{\partial x_D^2} = \gamma_L^{IN} \frac{\partial P'_D}{\partial t_D}, & x_D \in \left(0, x_D^{BL}\right) , \\ P'_D\left(x_D, t_D = 0\right) = 0 & \text{(I.C.)} , \\ \lim_{x_D \to 0}\left(\frac{\partial P'_D}{\partial x_D}\right) = -\frac{1}{\lambda_{TD}^{IN}} & \text{(I.B.C.)} . \end{cases}$$

The equations for the outer region are

$$\begin{cases} \frac{\partial^2 P'_D}{\partial x_D^2} = \hat{\gamma}_L \frac{\partial P'_D}{\partial t_D}, & x_D \in \left(x_D^{BL}, 1\right) , \\ P'_D\left(x_D, t_D = 0\right) = 0 & \text{(I.C.)} , \\ P'_D\left(x_D = 1, t_D\right) = 0 & \text{(E.B.C.)} . \end{cases}$$

The continuity of pressure and total flow rate at the interface of the two regions are used to close the problem.

$$\lim_{x_D \to x_D^{BL-}} P'_D\left(x_D, t_D\right) = \lim_{x_D \to x_D^{BL+}} P'_D\left(x_D, t_D\right)$$
$$\left(\lambda_{TD}^{IN} \frac{\partial P_D(x_D, t_D)}{\partial x_D}\right)_{x_D^{BL-}} = \left(\frac{\partial P_D(x_D, t_D)}{\partial x_D}\right)_{x_D^{BL+}} .$$

The shock position $x_D^{BL} = x_D^{BL}\left(t_D\right)$ characterizes a moving internal condition. However, as the speed of this boundary is small, we may use a quasi-stationary assumption, in which the effect of a moving interface is neglected in the solution. However, the interface position is updated every time t_D in order to evaluate the dimensionless pressure $P_D\left(x_D, t_D\right)$.

1.2.2.1 Solution by the Laplace Transform

The quasi-stationary hypothesis allows one to solve the two-region problem by the Laplace transform. Applying the transform in the PDE and in both boundary conditions and using the initial condition, the system can be written for the inner zone as

$$\begin{cases} \frac{\partial^2 \bar{P}'_D}{\partial x_D^2} = \gamma_L^{IN} u \bar{P}'_D, & x_D \in \left(0, x_D^{BL}\right) \ , \\ \lim_{x_D \to 0} \left(\frac{\partial \bar{P}'_D}{\partial x_D}\right) = -\frac{1}{u\lambda_{TD}^{IN}} & \text{(I.B.C.)} \end{cases}$$

and for the outer zone as

$$\begin{cases} \frac{\partial^2 \bar{P}'_D}{\partial x_D^2} = \hat{\gamma}_L u \bar{P}'_D, & x_D \in \left(x_D^{BL}, 1\right) \ , \\ \bar{P}'_D \left(x_D = x_{Ds}, u\right) = 0 & \text{(E.B.C.)} \ . \end{cases}$$

The coupling condition in Laplace's domain is given by

$$\begin{array}{c} \lim_{x_D \to x_D^{BL-}} \bar{P}'_D \left(x_D, u\right) = \lim_{x_D \to x_D^{BL+}} \bar{P}'_D \left(x_D, u\right) \\ \left(\lambda_{TD}^{IN} \frac{\partial \bar{P}'_D(x_D, u)}{\partial x_D}\right)_{x_D^{BL-}} = \left(\frac{\partial \bar{P}'_D(x_D, u)}{\partial x_D}\right)_{x_D^{BL+}} \end{array} .$$

The general solution is

$$\begin{array}{ll} \bar{P}'_D \left(x_D, u\right) = A_0 e^{\sqrt{\gamma_L^{IN} u} x_D} + A_1 e^{-\sqrt{\gamma_L^{IN} u} x_D}, & \text{for } x_D \in \left(0, x_D^{BL}\right) \ , \\ \bar{P}'_D \left(x_D, u\right) = A_2 e^{\sqrt{\hat{\gamma}_L u} x_D} + A_3 e^{-\sqrt{\hat{\gamma}_L u} x_D}, & \text{for } x_D \in \left(x_D^{BL}, 1\right) \ . \end{array}$$

Applying the boundary and coupling conditions, it is possible to write the following system of equations:

$$\begin{pmatrix} 1 & -1 & 0 & 0 \\ 0 & 0 & e^{\hat{\alpha}_L x_{Ds}} & e^{-\hat{\alpha}_L x_{Ds}} \\ e^{\alpha_L^{IN} x_D^{BL}} & e^{-\alpha_L^{IN} x_D^{BL}} & -e^{\hat{\alpha}_L x_D^{BL}} & -e^{-\hat{\alpha}_L x_D^{BL}} \\ \lambda_{TD}^{IN} \alpha_L^{IN} e^{\alpha_L^{IN} x_D^{BL}} & -\lambda_{TD}^{IN} \alpha_L^{IN} e^{-\alpha_L^{IN} x_D^{BL}} & -\hat{\alpha}_o e^{\hat{\alpha}_L x_D^{BL}} & \hat{\alpha}_o e^{-\hat{\alpha}_L x_D^{BL}} \end{pmatrix} \begin{pmatrix} A_0 \\ A_1 \\ A_2 \\ A_3 \end{pmatrix} = \begin{pmatrix} -\frac{1}{\lambda_{TD}^{IN}} \frac{1}{u\alpha_L^{IN}} \\ 0 \\ 0 \\ 0 \end{pmatrix} ,$$

with $\alpha_L^{IN} = \sqrt{\gamma_L^{IN} u}$ and $\hat{\alpha}_L = \sqrt{\hat{\gamma}_L u}$. The coefficients A_0, A_1, A_2, and A_3 are calculated through

$$A_0 = \frac{1}{\lambda_{TD}^{IN}\alpha_L^{IN} u}\left(\frac{2\lambda_{TD}^{IN}\alpha_L^{IN}\left(e^{-\hat{\alpha}_L x_D^{BL}} - e^{\hat{\alpha}_L\left(x_D^{BL}-2\right)}\right) - e^{-\alpha_L^{IN} x_D^{BL}}\Omega_L}{2\cosh\left(\alpha_L^{IN} x_D^{BL}\right)\Omega_L}\right) ,$$

$$A_1 = \frac{1}{\lambda_{TD}^{IN}\alpha_L^{IN} u}\left(\frac{e^{\alpha_L^{IN} x_D^{BL}}\Omega_L + 2\lambda_{TD}^{IN}\alpha_L^{IN}\left(e^{-\hat{\alpha}_L x_D^{BL}} - e^{\hat{\alpha}_L\left(x_D^{BL}-2\right)}\right)}{2\cosh\left(\alpha_L^{IN} x_D^{BL}\right)\Omega_L}\right) ,$$

$$A_2 = -\frac{2e^{-2\hat{\alpha}_L}}{u\Omega_L} ,$$

$$A_3 = \frac{2}{u\Omega_L} ,$$

in which

$$\Omega_L = \left(\hat{\alpha}_L + \lambda_{TD}^{IN}\alpha_L^{IN}\right)\left(e^{\left(\alpha_L^{IN}-\hat{\alpha}_o\right)x_D^{BL}} + e^{\hat{\alpha}_L\left(x_D^{BL}-2\right)-\alpha_L^{IN}x_D^{BL}}\right) ,$$
$$+ \left(\hat{\alpha}_L - \lambda_{TD}^{IN}\alpha_L^{IN}\right)\left(e^{-\left(\alpha_L^{IN}+\hat{\alpha}_L\right)x_D^{BL}} + e^{\hat{\alpha}_L\left(x_D^{BL}-2\right)+\alpha_L^{IN}x_D^{BL}}\right) .$$

The coefficients A_0, A_1, A_2, and A_3 are time dependent because the interface position between the regions moves. Finally, we can apply Darcy's law (Eq. 1.2) in the two-zone pressure solution and obtain the approximated flow-rate profile

$$\bar{q}_{DC}\left(x_D, u\right) = \begin{cases} -\lambda_{TD}^{IN}\sqrt{\gamma_L^{IN} u}\, e^{\sqrt{\gamma_L^{IN} u}\, x_D} A_0 + \lambda_{TD}^{IN}\sqrt{\gamma_L^{IN} u}\, e^{-\sqrt{\gamma_L^{IN} u}\, x_D} A_1 \\ \qquad \text{for } x_D < x_D^{BL} , \\ -\sqrt{\hat{\gamma}_L u}\, e^{\sqrt{\hat{\gamma}_L u}\, x_D} A_2 + \sqrt{\hat{\gamma}_L u}\, e^{-\sqrt{\hat{\gamma}_L u}\, x_D} A_3 \\ \qquad \text{for } x_D > x_D^{BL} . \end{cases} \tag{1.13}$$

These equations are inverted to real space using Stehfest's algorithm [GS70]. When the water front position reaches the external core face, Eq. 1.13 for $x_D < x_D^{BL}$ is still valid; however, the terms γ_L^{IN} and λ_{TD}^{IN} must be averaged inside the core domain ($x_D \in (0, 1)$).

1.3 Model Validation

In this section, we apply the developed solution for a set of typical laboratory core flood experiment parameter sets (Table 1.1). The relative permeability curves were generated using the Corey model [C56],

$$\begin{cases} k_{rw} = k_{rw}^{S_{or}^w} \, (S_{nw})^{n_w} \, , \\ k_{ro} = k_{ro}^{S_{wi}} \, (S_{no})^{n_o^w} \, , \end{cases}$$

using properties shown in Table 1.2 and Fig. 1.3. The mobility ratio is given by $M = \frac{\hat{\lambda}_w}{\hat{\lambda}_o}$, where $\hat{\lambda}_w$ and $\hat{\lambda}_o$ denote the water mobility at residual oil saturation and the oil mobility at irreducible water saturation. For the data shown in Table 1.2, we have $M = 1.875$.

All solutions discussed in this section are compared to numerical results.

1.3.1 Injection Schedule 1

The first case analyzed is an isochronal schedule composed of three increasing injection flow rates followed by a falloff (Table 1.3). To generate the approximate solution, the first step is solving the incompressible problem (Eq. 1.11) using the fractional flow shown in Fig. 1.3. Comparing the incompressible solution with the

Table 1.1 Typical rock and fluid properties for core flood experiments

Core length	$L = 15$	[cm]
Cross-sectional area	$A = 11.4$	[cm^2]
Porosity	$\phi = 0.1$	[-]
Absolute permeability	$K = 200$	[mD]
Initial injection rate	$q_T^0 = 0.54$	[cm^3/min]
Water viscosity	$\mu_w = 1.0$	[cp]
Oil viscosity	$\mu_o = 5.0$	[cp]
Rock compressibility	$c_r = 9.8E - 6$	[1/Kgf/cm2]
Water compressibility	$c_w = 1.0E - 6$	[1/Kgf/cm2]
Oil compressibility	$c_o = 4.0E - 5$	[1/Kgf/cm2]

Table 1.2 Relative permeability curves parameters

$S_{wi} = 0.20$
$k_{ro}^{S_{wi}} = 0.80$
$S_{or}^w = 0.20$
$k_{rw}^{S_{or}^w} = 0.30$
$n_w = 2.2$
$n_o^w = 2.0$

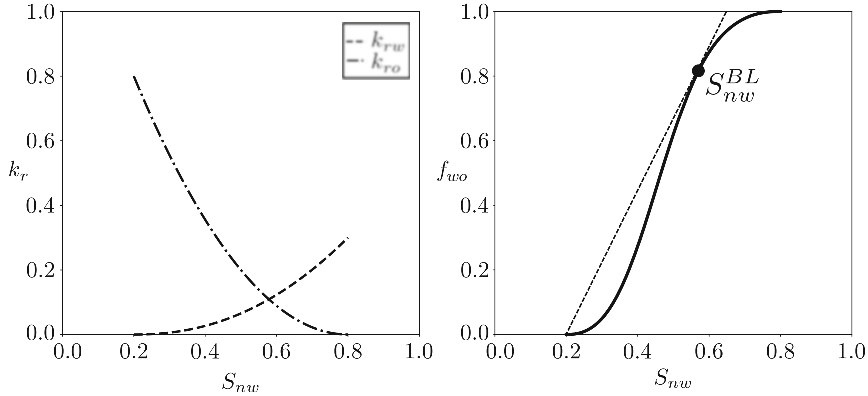

Fig. 1.3 Relative permeability curves (left) and water fraction flow curve (right) for data shown in Tables 1.1 and 1.2

Table 1.3 Injection schedule 1

t_D	q_D^{INJ}
0.00–0.05	1.0
0.05–0.10	2.0
0.10–0.15	3.0
0.15–0.20	0.0

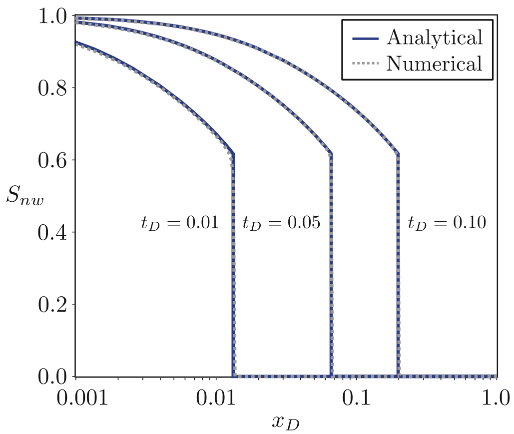

Fig. 1.4 Analytical and numerical saturation profiles for schedule 1

numerical compressible solution (Fig. 1.4), it can be observed that the saturation profile matches for different injection times.

Once we have the saturation profile, we can solve Eq. 1.13 and obtain an approximate flow rate. In Fig. 1.5, three different Δt_D after the first flow-rate change ($t_D = 0.05$) are compared. Note that the greatest difference between solutions

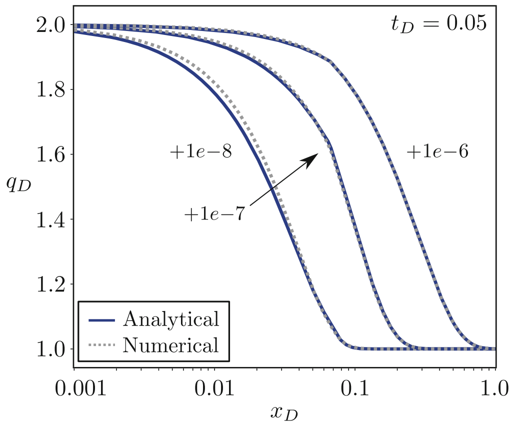

Fig. 1.5 Analytical and numerical flow-rate profile for different Δt_D after $t_D = 0.05$

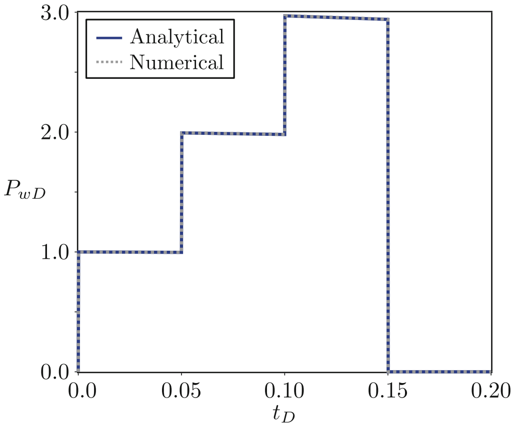

Fig. 1.6 Analytical and numerical P_{wD} solution for schedule 1

appears at small times ($\Delta t_D = 1e^{-8}$). After $\Delta t_D = 1e^{-7}$, the solutions present close agreement. Using the calculated λ_{TD} and q_D, it is possible to integrate Equation 1.9 and obtain the final solution (Fig. 1.6).

1.3.2 Injection Schedule 2

The second case changes the injection flow rate schedule (Table 1.4) using the same reservoir properties (Tables 1.1 and 1.2). Schedule 2 is composed of three isochronal decreasing flow rates, followed by a falloff. Figures 1.7 and 1.8 present the saturation and flow-rate profiles compared with the compressible numerical solutions. The presented profiles are calculated at three different Δt_D after the falloff

Table 1.4 Injection schedule 2

t_D	q_{Di}
0.00–0.05	1.0
0.05–0.10	2/3
0.10–0.15	1/3
0.15–0.20	0.0

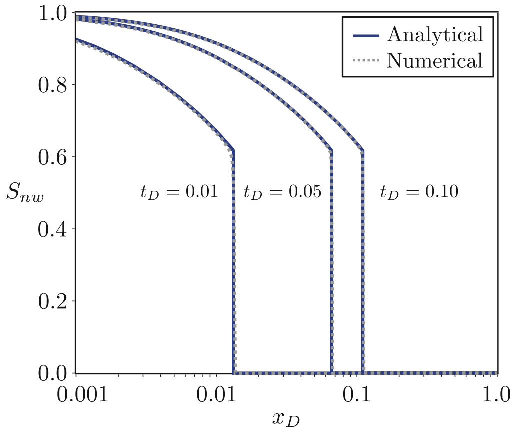

Fig. 1.7 Analytical and numerical saturation profiles for different t_D for schedule 2

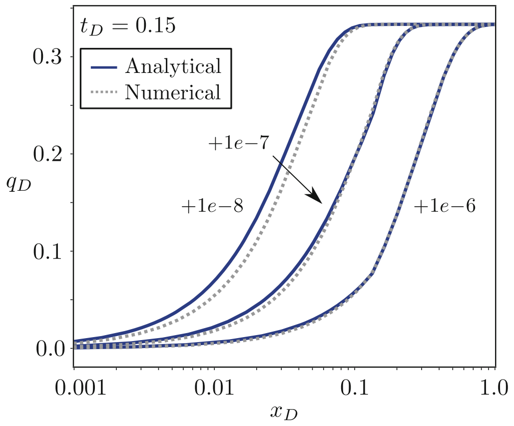

Fig. 1.8 Analytical and numerical flow-rate profile for different Δt_D after $t_D = 0.15$

($t_D = 0.15$). It can be noted that both solutions agree and can be used to build the pressure solution of the original problem (Fig. 1.9). Note that our approximation of P_{wD} agrees with numerical simulation for all flow-rate steps.

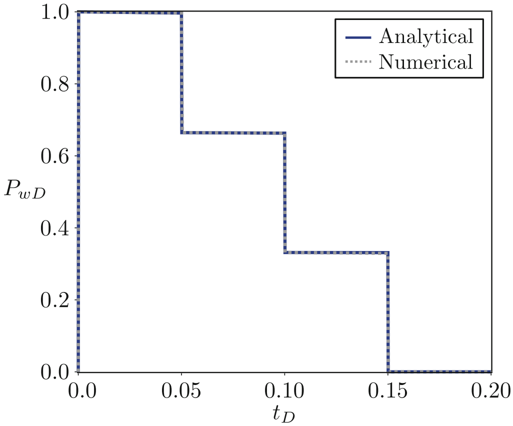

Fig. 1.9 Analytical and numerical P_{wD} solution for schedule 2

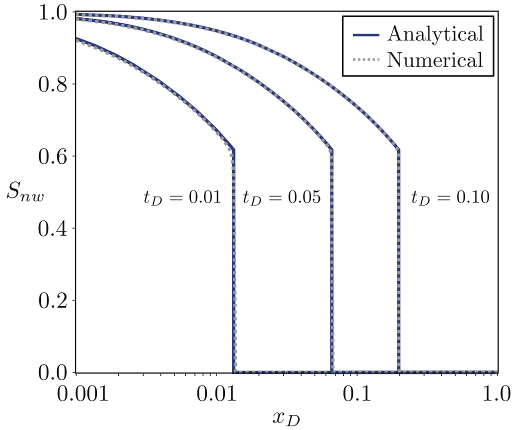

Fig. 1.10 Analytical and numerical saturation profile for different t_D for a more compressible system

1.3.3 Compressibility Effect

Schedule 1 (Table 1.3) was used to analyze the compressibility effects in the results ($c_r = 1.0E - 2$ 1/MPa and $c_o = 4.0E - 3$ 1/Kgf/cm2 keeping all other properties constant. Even increasing the compressibility by a factor of 100, the incompressible and compressible saturation profiles still match (Fig. 1.10). As this system is much more compressible, it is expected that the flow rate propagates slower in the reservoir (Fig. 1.11). It can be noted that both solutions agree after $\Delta t_D = 1e^{-6}$. The pressure solution is presented in Fig. 1.12 showing the excellent agreement with numerical compressible simulation.

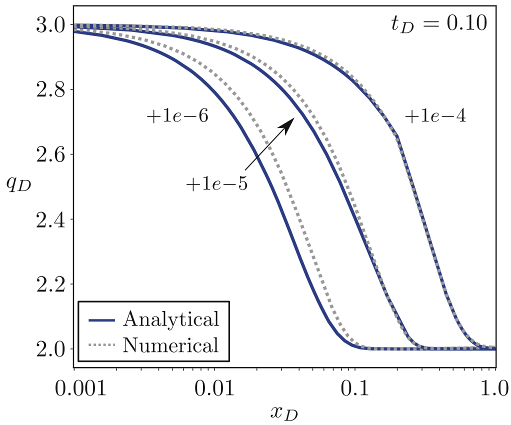

Fig. 1.11 Analytical and numerical flow-rate profile for different Δt_D after $t_D = 0.10$

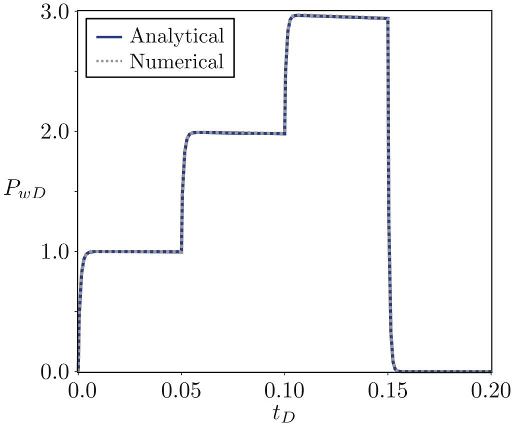

Fig. 1.12 Analytical and numerical P_{wD} solution for a more compressible system

1.4 Conclusion

This work presents a new solution for the pressure drop along a linear porous medium considering immiscible two-phase oil displacement and a step-rate variable boundary condition. The solution is calculated based on two main hypothesis:

1. The mobility profile can be determined by the incompressible problem solution.
2. The total flow rate can be calculated by a dual-zone compressible problem.

The model was tested for two different flow rate schedules, and the results were compared to numerical solutions with excellent agreement. The analytical solution built in this work can be used to model laboratory core flood experiments.

Acknowledgments The authors acknowledge Universidade Estadual do Norte Fluminense (UENF) for financial support. This study was also financed in part by the Coordenação de Aperfeiçoamento de Pessoal de Nível Superior—Brasil (CAPES)—Finance Code 001.

References

[AK89] Abbaszadeh, M., & Kamal, M.: Pressure-transient testing of water-injection wells. SPE Reserv. Eng. **4**(01), 115–124 (1989). Society of Petroleum Engineers (SPE). https://doi.org/10.2118/16744-pa

[AS09] Azevedo, A.V., Souza, A.J., Furtado, F., Marchesin, D., Plohr, B.: The solution by the wave curve method of three-phase flow in virgin reservoirs. Trans. Porous Media **83**(01), 99–125 (2009). Springer Science and Business Media LLC. https://doi.org/10.1007/s11242-009-9508-9

[BH90] Bratvold, R.B., Horne, R.N.: Analysis of pressure-falloff tests following cold-water injection. SPE Form. Evaluation **5**(03), 293–302 (1990). Society of Petroleum Engineers (SPE). https://doi.org/10.2118/18111-pa

[BL42] Buckley, S., Leverett, M.: Mechanism of fluid displacement in sands. Trans. AIME **146**(01), 107–116 (1942). Society of Petroleum Engineers (SPE). https://doi.org/10.2118/942107-g

[BTR98] Banerjee, R., Thompson, L.G., Reynolds, A.C.: Injection/falloff testing in heterogeneous reservoirs. SPE Reser. Evaluation Eng. **1**(06), 519–527 (1998). Society of Petroleum Engineers (SPE). https://doi.org/10.2118/52670-pa

[CAFM16] Castañeda P., Abreu, E., Furtado, F., Marchesin, D.: On a universal structure for immiscible three-phase flow in virgin reservoirs, Comput. Geosci. **20**(01), 171–185 (2016). Springer Science and Business Media LLC. https://doi.org/10.1007/s10596-016-9556-5

[C56] Corey, A.T., Rathjens, C.H., Henderson, J.H., Wyllie, M.R.J.: Three-phase relative permeability. J. Petroleum Technol. **8**(11), 63–65 (1956). Society of Petroleum Engineers (SPE). https://doi.org/10.2118/737-g

[FS59] Fayers, F.J., Sheldon, J.W.: The effect of capillary pressure and gravity on two-phase fluid flow in a porous medium. Trans. AIME **216**(01), 147–155 (1959). Society of Petroleum Engineers (SPE). https://doi.org/10.2118/1089-g

[GF97] Guzmán, R.E., Fayers, F.J.: Mathematical properties of three-phase flow equations. SPE J. **2**(03), 291–300 (1997). Society of Petroleum Engineers (SPE). https://doi.org/10.2118/35154-pa

[GS70] Stehfest, H.: Algorithm 368: numerical inversion of laplace transforms. Commun. ACM **13**, 47–49 (1970)

[HRM58] Hazebroek, P., Rainbow, H., Matthews, C.S.: Pressure fall-off in water injection wells. Trans. AIME **213**(01), 250–260 (1958). Society of Petroleum Engineers (SPE). https://doi.org/10.2118/925-g

[IMPT92] Isaacson, E.L., Marchesin, D., Plohr, B.J., Temple, J.B.: Multiphase flow models with singular Riemann problems. Mat. Apl. Comput. **11**(02), 147–166 (1992). Sociedade Brasileira de Matemática Aplicada e Computacional

[JBN59] Johnson, E.F., Bossler, D.P., Neumann, V.O.: Calculation of relative permeability from displacement experiments. Trans. AIME **216**, 370–372 (1959). Society of Petroleum Engineers (SPE), SPE-1023G

[KMJ72] Kazemi, H., Merrill, L.S., Jargon, J.R.: Problems in interpretation of pressure fall-off tests in reservoirs with and without fluid banks. J. Petrol. Technol. **24**(09), 1147–1156 (1972). Society of Petroleum Engineers (SPE). https://doi.org/10.2118/3696-pa

[L07] Liu, T.: Hyperbolic and Viscous Conservation Laws. CBMS-NSF Regional Conference Series in Applied Mathematics, vol. 01. SIAM, Philadelphia (2007)

[L57] Lax, P.D.: Hyperbolic systems of conservation laws II. Commun. Pure Appl. Math. **10**(04), 537–566 (1957). Wiley. https://doi.org/10.1002/cpa.3160100406

[O57] Oleinik, O.A.: On the uniqueness of the generalized solution of the Cauchy problem for a non-linear system of equations occurring in mechanics. Uspekhi Mat. Nauk **12**, 169–176 (1957)